CHEMISTRY
A EUROPEAN JOURNAL

DOI: 10.1002/chem.200601534

Reversible Transformation of Zn^{II} Coordination Geometry in a Single Crystal of Porous Metal-Organic Framework $[Zn_3(ntb)_2(EtOH)_2]\cdot 4EtOH$

Myunghyun Paik Suh,* Young Eun Cheon, and Eun Young Lee[a]

Abstract: A 3D porous metal-organic framework $[Zn_3(ntb)_2(EtOH)_2]_n\cdot 4n$EtOH (**1**) that generates 1D channels of honeycomb aperture has been prepared by the solvothermal reaction of $Zn(NO_3)_2\cdot 6H_2O$ and 4,4′,4″-nitrilotrisbenzoic acid (H_3NTB) in EtOH at 110 °C. Framework **1** exhibits reversible single-crystal-to-single-crystal transformations upon removal and rebinding of the coordinating EtOH as well as the EtOH guest molecules, which give rise to desolvated crystal $[Zn_3(ntb)_2]_n$ (**1′**) and resolvated crystal $[Zn_3(ntb)_2(EtOH)_2]_n\cdot 4n$EtOH (**1″**). The X-ray structures indicate that 3D host framework is retained during the transformations from **1** to **1′** and from **1′** to **1″**, but the coordination geometry of Zn^{II} ions changes from/to trigonal bipyramid to/from tetrahedron, concomitant with the rotational rearrangement of a carboxylate plane of the NTB^{3-} relative to its associated phenyl ring. To retain the single crystal integrity, extensive cooperative motions must exist between the molecular components throughout the crystal. Framework **1′** exhibits permanent porosity, thermal stability up to 400 °C, and blue luminescence, and high storage capabilities for N_2, H_2, CO_2, and CH_4.

Keywords: coordination modes · gas sorption · metal–organic frameworks · microporous materials

Introduction

Metal-organic open frameworks (MOFs) have diverse potential applications as new materials in gas storage,[1–5] molecular adsorption and separation processes,[6–12] ion-exchange,[13–15] catalysis,[16–18] sensors,[19–21] and fabrication of metal nanoparticles.[22,23] In particular, the MOFs that transform their structures reversibly with retention of the single crystallinity in response to external stimuli are important for the development of new and technologically useful materials including devices and sensors. For a general applicability, MOFs should have permanent porosity and high thermal stability. However, when MOFs are prepared, they often contain metal ions that are coordinated to solvent molecules; also, the open structures commonly collapse on removal of the coordinating solvent molecules. Therefore, the chance of finding the MOFs that exhibit permanent porosity after removal of coordinating solvent molecules is extremely rare.[24–28] MOFs that released the coordinating solvent molecules are seldom characterized by the X-ray crystallography due to the loss of single crystallinity.[28–30] Despite the lack of X-ray crystal structures, however, it has been generally believed that MOFs generate vacant coordination sites when coordinating solvent molecules are removed from the metal ions; such MOFs have been anticipated to enhance the hydrogen storage capability.[27,31–33]

Here we report, based on the single-crystal X-ray structures, that a porous 3D metal-organic framework $[Zn_3(ntbB)_2(EtOH)_2]_n\cdot 4n$EtOH (**1**) changes the coordination geometry of Zn^{II} ions reversibly from/to trigonal bipyramid to/from tetrahedron (both of which are the thermodynamically most stable coordination forms) upon removal and rebinding of coordinating solvent molecules rather than simply generating vacant coordination sites. Despite this coordination flexibility of metal ions, the host framework structure as well as single crystallinity is retained during the desolvation and resolvation processes. The desolvated solid $[Zn_3(ntb)_2]_n$ (**1′**), which lost a coordinating EtOH as well as guest EtOH molecules, exhibits permanent porosity (Langmuir surface area = 419 $m^2 g^{-1}$; pore volume = 0.15 $cm^3 cm^{-3}$) and remarkable gas storage capabilities for N_2, H_2, CO_2, and CH_4.

[a] Prof. M. P. Suh, Y. E. Cheon, E. Y. Lee
Department of Chemistry, Seoul National University
Seoul 151-747 (Republic of Korea)
Fax: (+82) 886-8516
E-mail: mpsuh@snu.ac.kr

Supporting information for this article is available on the WWW under http://www.chemeurj.org/ or from the author.

Results and Discussion

Preparation and X-ray structure of 1: A metal-organic open framework $[Zn_3(ntb)_2(EtOH)_2]_n \cdot 4n$EtOH (**1**) has been prepared by the solvothermal reaction of $Zn(NO_3)_2 \cdot 6H_2O$ and H_3NTB in EtOH at 110 °C. Previously, we reported a different porous framework $[Zn_4O(ntb)_2]_n \cdot 3nDEF\cdot n$EtOH (**2**; DEF = diethylformamide), which was prepared from the same starting materials but in the different solvent system, DEF/EtOH/H_2O (5:3:2 v/v/v).[2] Upon desolvation of **2**, the framework structure changed as a result of the rotation of molecular components, but upon resolvation with EtOH, pyridine, or benzene, **2** was regenerated. However, when the same solvothermal reaction was carried out in EtOH in the present study, we obtained framework **1**, which has an X-ray structure and properties completely different from those of **2**.

The X-ray crystal structure of **1** is shown in Figure 1. In **1**, each NTB^{3-} coordinates six Zn^{II} ions because every carboxylate group behaves as a bidentate to bind two Zn^{II} ions. The NTB^{3-} looks like a propeller since the average dihedral angle between the phenyl rings is 71.3(1)°. The central nitrogen of NTB^{3-} exhibits sp^2 hybridization, showing C-N-C average angles of 119.1(2)° and a unusually short N–C bond lengths [av 1.423(3) Å]. There are crystallographically independent two Zn^{II} centers: Zn1 and Zn2. They form a Zn_3 cluster unit in the sequence of Zn1–Zn2–Zn1 by binding to the carboxylate groups of NTB^{3-} with a twofold rotational symmetry at Zn2 (Figure 1a). Zn1 shows a distorted trigonal bipyramidal (tbp) coordination geometry, being coordinated with four carboxylate oxygen atoms (O2, O4, O5, and O6) of four different NTB^{3-} ligands and with an oxygen atom (O7) of EtOH at the axial site of tbp geometry. Although alcohols are extremely weak ligands, there are a few reports on MeOH coordination to Zn^{II} ion.[25,34] In **1**, a EtOH molecule coordinates a Zn^{II} ion with the Zn–O bond length of 2.261(5) Å, which is significantly longer than Zn1–O-(NTB^{3-}) bond lengths [av 1.992(2) Å]. Zn2 shows distorted tetrahedral coordination geometry, being coordinated with four oxygen atoms, each from four different NTB^{3-} ligands. The Zn_3 cluster units are connected repeatedly by O5 and O6 of NTB^{3-} to form a 1D chain that extends along the [101] direction (Figure 1a).

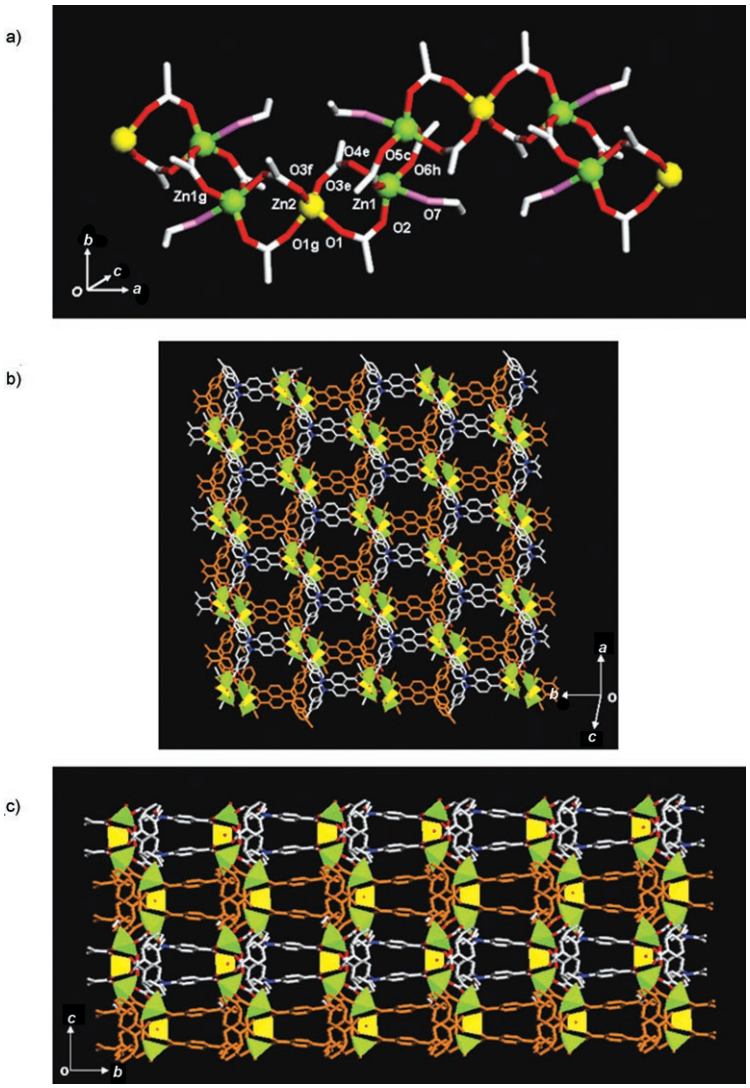

Figure 1. X-ray structure of **1**. a) A Zn^{II} 1D chain formed of Zn1–Zn2–Zn1 cluster units, which extends along the [101] direction. Symmetry operations: a: $(-x, y, -z+0.5)$, b: $(x+0.5, y-0.5, z)$, c: $(-x+0.5, y-0.5, -z+0.5)$, d: $(-x, -y+1, -z)$, e: $(x, -y+1, z+0.5)$, f: $(x-0.5, y-0.5, z)$, g: $(-x-0.5, y-0.5, -z-0.5)$, h: $(x+0.5, -y+0.5, z+0.5)$. b) View on the (101) plane, showing the bilayers of honeycomb aperture with Zn_3 pillars. c) View on the *bc* plane, showing that the bilayers are linked in a staggered manner to form a 3D framework. Guest EtOH molecules are omitted for clarity. Color scheme: Zn (td), yellow; Zn (tbp), green; N, blue; O, red; O of coordinating EtOH, pink; C of two different bilayers, white and brown.

One of the Zn1 atoms of a Zn_3 cluster unit and the nitrogen atom of NTB^{3-} are located alternately at the corners of hexagonal compartments, which gives rise to a 2D honeycomb-like layer extending parallel to the (001) plane (Figure 1b). Since each of the two Zn1 atoms in a Zn_3 cluster unit is involved in the formation of the 2D layer, a bilayer

with Zn_3 pillars is formed. The bilayers with Zn_3 pillars are linked infinitely through O5 and O6 atoms of the NTB^{3-} (Figure 1c), which gives rise to a 3D framework generating 1D channels of honeycomb aperture. The edge length of a hexagonal compartment is 8.04 Å, and the effective size of the hexagonal pore is about 7.72 Å. The channels are occupied by EtOH molecules coordinating Zn1 ions as well as EtOH guest molecules. The void volumes of **1** with and without coordinating EtOH molecules are 39 and 48%, respectively, as estimated by PLATON.[35] In the 3D framework, two phenyl rings of each NTB^{3-} are involved in the edge-to-face π–π interactions with those of the adjacent layer {the shortest C–C distance: C10–C16 ($-x-0.5$, $-y+1.5$, $-z$), 3.828(6) Å; dihedral angle, 78.9(2)°}. Thermogravimetric analysis of **1** reveals 22% weight loss at 25–116°C (see Supporting Information), which corresponds to all coordinating EtOH as well as EtOH guest molecules (calcd 22.6%). The host framework is thermally stable up to 400°C, as evidenced by the temperature dependent XRPD patterns (see Supporting Information). Solid **1** and its desolvated solid (**1′**) exhibit luminescence at $\lambda_{max}=$ 482 and 475 nm, respectively, upon photo-irradiation at 340 nm (see Supporting Information).

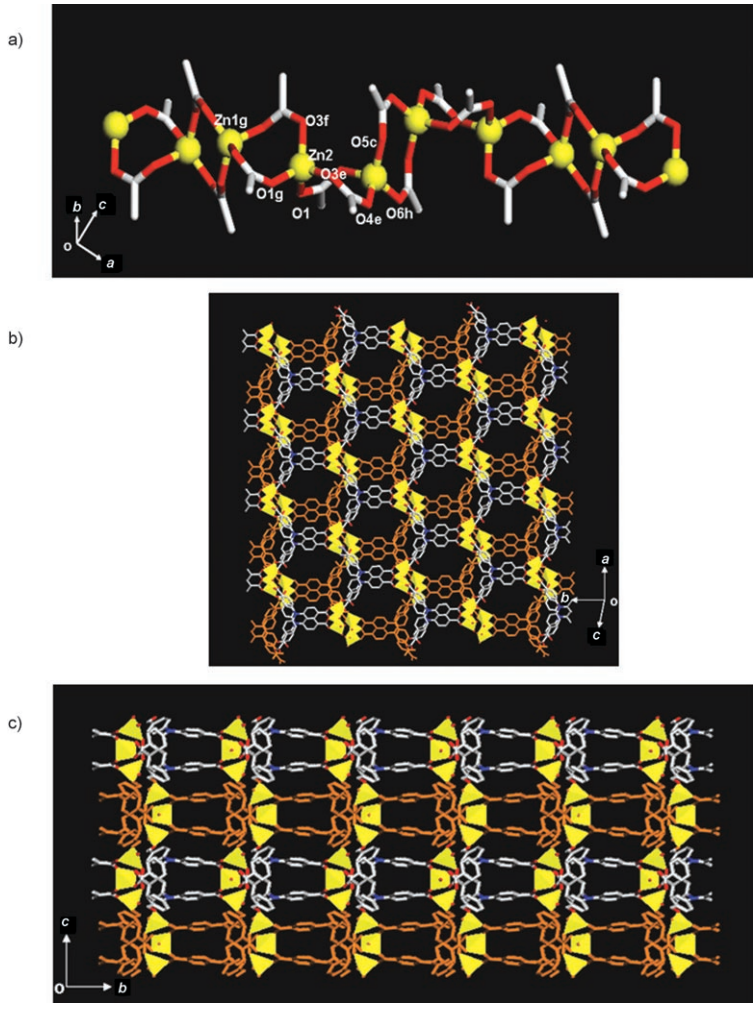

Figure 2. X-ray crystal structure of $[Zn_3(ntb)_2]_n$ (**1′**). a) The Zn^{II} 1D chain extending along the [101] direction. Symmetry operations: a: ($-x$, y, $-z+0.5$), b: ($x+0.5$, $y-0.5$, z), c: ($-x+0.5$, $y-0.5$, $-z+0.5$), d: ($-x$, $-y+1$, $-z$), e: (x, $-y+1$, $z+0.5$), f: ($x-0.5$, $y-0.5$, z), g: ($-x-0.5$, $y-0.5$, $z-0.5$), h: ($x+0.5$, $-y+0.5$, $z+0.5$), i: ($-x$, $-y+1$, $-z+1$). b) View on the (101) plane, showing bilayers of the honeycomb aperture formed of Zn_3 pillars. c) View on the *bc* plane, showing that the bilayers are linked in a staggered manner to form a 3D framework. Color schemes are the same as in Figure 1.

Single-crystal-to-single-crystal transformations of 1: These transformations involve reversible coordination geometry changes of Zn^{II} upon removal and rebinding of coordinating EtOH molecules. The X-ray crystal structures of MOFs, where coordinating solvent molecules are removed, are extremely rare.[28–30] This is because single-crystallinities and/or open framework structures are commonly destroyed when coordinating solvent molecules are removed from MOFs. Contrary to the common MOFs, when crystal **1** was heated at 150°C under vacuum for 5 h to remove the coordinating EtOH as well as the guest EtOH molecules, $[Zn_3(ntb)_2]_n$ (**1′**) was obtained with retention of the single crystallinity. The X-ray crystal structure of **1′** reveals that the framework structure and the packing mode of **1** are retained (Figure 2), but the molecular rearrangements involving alteration of coordination geometry of Zn1 occur in **1′**. The coordination geometry of Zn1 changes from a trigonal bipyramid to a coordinatively saturated tetrahedron, instead of a trigonal pyramid that contains a vacant coordination site at the apical position (Scheme 1). In par-

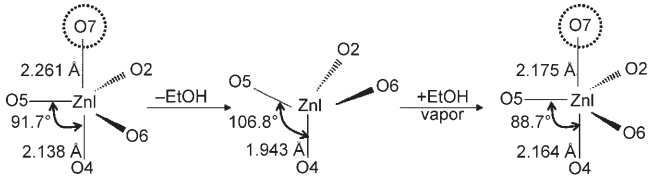

Scheme 1. Rearrangement of coordination geometry of Zn1 on removal and rebinding of a coordinating EtOH molecule.

ticular, the O4-Zn1-O5 angle increases from 91.7(2) to 106.8(1)°, and the bond length of Zn1−O4 decreases from 2.138(3) to 1.943(2) Å. Furthermore, the carboxylate plane of O5-C15-O6, which connects two Zn_3 cluster units via terminal Zn1 atoms, undergoes a rotational motion relative to its associated phenyl ring, and alters the dihedral angle between them from 8.7(8) to 17.7(5)° (Figure 3a).

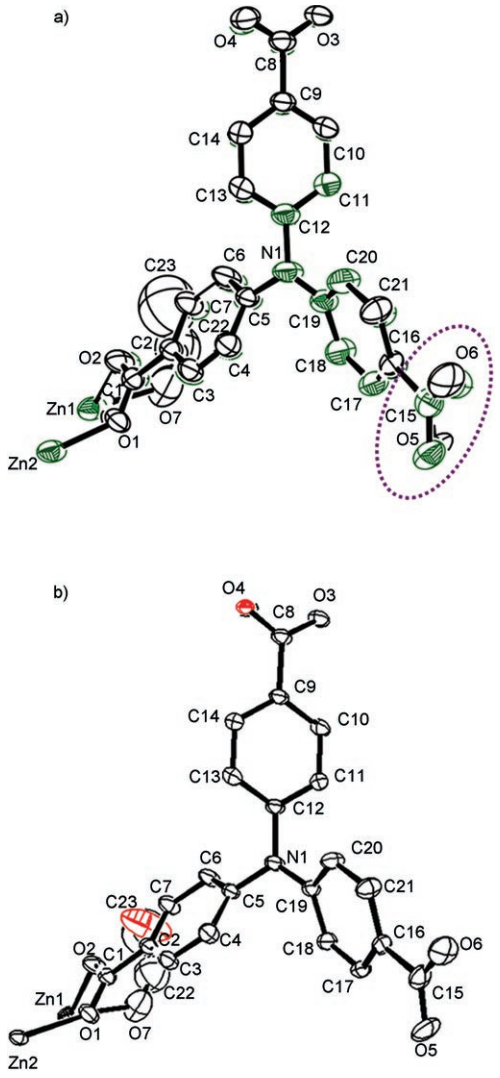

Figure 3. Superimposition of the crystallographic asymmetric units. a) Original crystal **1** (black) and desolvated crystal **1′** (green). Rotation of O5-C15-O6 plane in **1′** is depicted in dotted circle. b) Original crystal **1** (black) and resolvated crystal **1″** (red).

Interestingly, this crystal dynamics are reversible. When desolvated crystal **1′** is exposed to EtOH vapor for 3 h, resolvated crystal **1″** results. The X-ray crystal structure of **1″** indicates that the original structure of **1** is restored (Figure 3b). That is, even though Zn1 of **1′** is in a coordinatively saturated tetrahedron geometry, it provides a coordination site for the EtOH molecule and rearranges to a trigonal bipyramidal coordination geometry. In the transformation of **1′** to **1″**, the O4-Zn1-O5 angle decreases from 106.8(1) to 88.7(2)° and the bond length of Zn1−O4 increases to 2.164(3) Å. In addition, the carboxylate plane of O5-C15-O6 undergoes a reverse rotational motion with respect to its associated phenyl ring to restore the structure of **1**. In short, the single crystal transformations of **1** → **1′** → **1″** involve dynamic motions altering the coordination geometry of Zn^{II} from/to trigonal bipyramid to/from tetrahedron as well as the rotation of a carboxylate plane relative to its associated phenyl ring of NTB^{3-}. In order for the material to retain its single crystal integrity, extensive cooperative movements must exist between the molecular components throughout the crystal.

There have been only three reports so far for the X-ray crystal structures of the MOFs that released the coordinating solvent molecules from the metal ions.[28–30] In one MOF, the Cu^{II} ion loses a water molecule from the axial site of the square pyramidal geometry to provide the square planar Cu^{II} ion.[28] In the other MOF, the Co^{II} ion in the octahedral geometry loses a water molecule to give a square pyramidal Co^{II} ion.[29] In both cases, metal ions do not rearrange the coordination geometries and generate vacant coordination sites. However, in the third MOF, the Co^{II} ion in octahedral geometry rearranges to trigonal bipyramid upon removal of coordinating water molecules.[30] Based on the present results together with the previous reports, we suggest that the metal ions in MOFs transform their geometry to thermodynamically the most stable ones on release and uptake of the coordinating solvent molecules, instead of simply generating vacant coordination sites.

Gas-sorption properties: To verify the porosity of solid **1′** that lost the coordinating EtOH molecules as well as the EtOH guest molecules, gas sorption isotherms were measured with N_2, H_2, CO_2, and CH_4 (Figure 4 and Table 1). Solid **1′** adsorbs N_2 to show a reversible type I isotherm, which indicates a permanent microporosity. The gas sorption shows a little hysteresis between adsorption/desorption curves, suggesting a small amount of mesoporosity that is attributed to the intercrystalline voids.[36,37] The Langmuir surface area and pore volume, estimated by applying the Langmuir and Dubinin–Radushkevich equations, are 419 $m^2 g^{-1}$ and 0.14 $cm^3 g^{-1}$ (0.15 $cm^3 cm^{-3}$), respectively. A plot of pore size distribution based on Horvath–Kawazoe (HK) model[38] indicates that pore diameter of **1′** is about 4.6 Å (see Supporting Information).

Solid **1′** also adsorbs H_2 up to 1.0 wt% at 77 K and 1 atm (112 $cm^3 g^{-1}$ at STP, 4.7 H_2 molecules per formula unit). This weight percent of H_2 adsorption is not so high, but the density of adsorbed H_2 at 77 K and 1 atm (0.072 $g cm^{-3}$) is extraordinarily high and comparable to that (0.072 $g cm^{-3}$) of the supercritical fluid at 77 K and 478 atm.[39] Furthermore, a higher hydrogen sorption capacity is expected under higher pressures because the H_2 sorption isotherm of **1′** is not yet fully saturated at 1 atm.

Solid **1′** reveals high CO_2 and CH_4 sorption capacities. It adsorbs 29.7 wt% (6.75 $mmol g^{-1}$, 151 $cm^3 g^{-1}$ at STP) of

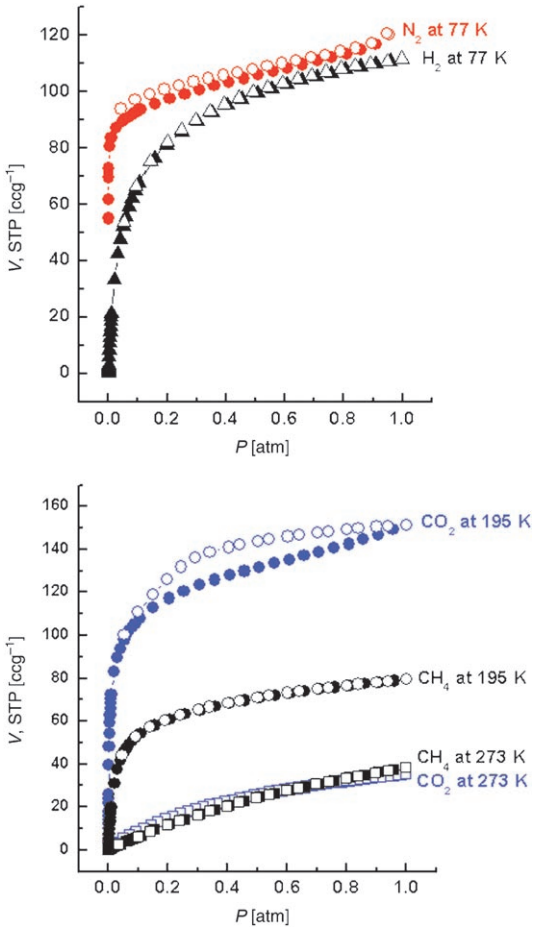

Figure 4. Gas-sorption isotherms for **1′**. a) N_2 and H_2 at 77 K. b) CO_2 (blue) and CH_4 (black) at 195 K (circle) and 273 K (square). $p_0(N_2)=$ 760 torr. Filled shapes, adsorption; open shapes, desorption.

Table 1. Gas-sorption data of **1′**.

Gas	T [K]	Langmuir surface area [$m^2 g^{-1}$]	mmol gas per g host[a]	wt % gas[a]	Volume %[b] [$cm^3 cm^{-3}$]
N_2	77	419	5.15	14.4	125
H_2	77		4.98	1.0	117
CO_2	195	559	6.75	29.7	159
CO_2	273		1.57	6.9	37
CH_4	195		3.55	5.7	83
CH_4	273		1.72	2.8	40

[a] Amounts of gas adsorbed; at $P=730$ Torr for N_2 and at $P=760$ Torr for all other gases. [b] Adsorbed gas volume divided by the density of **1′**.

CO_2 at 195 K and 1 atm, and 6.9 wt % (1.57 mmol g^{-1}, 35.3 $cm^3 g^{-1}$ at STP) of CO_2 at 273 K and 1 atm. For the CO_2 sorption data also a hysteresis exists between adsorption/desorption curves, which is attributed to the intercrystalline voids.[36,37] The gas isotherms for CH_4 indicate that **1′** stores CH_4 up to 5.7 wt % (3.55 mmol g^{-1}, 79.4 $cm^3 g^{-1}$ at STP) at 195 K, and 2.8 wt % (1.72 mmol g^{-1}, 38.5 $cm^3 g^{-1}$ at STP) at 273 K. These data are superior to those of other MOFs that stores CO_2 and CH_4.[40,41]

These gas sorption properties may be applied in gas storage and/or separation. For instance, **1′** can be applied in purification of H_2 since it has much higher adsorption capabilities for N_2 and CO_2 than H_2 in the low-pressure range. The removal of small amounts of contaminant gases from H_2 is important for the economical use of hydrogen as a fuel. In addition, it can be also applied in CO_2 removal from the natural gas since its adsorption capacity for CO_2 at 195 K is higher than that of CH_4.

Ethanol vapor sorption of 1′: The X-ray crystal data suggest that the transformation of **1′** to **1″** involves two types of EtOH binding: one is direct coordination to the metal ions and the other is inclusion in the channels. The EtOH vapor sorption isotherm indicates that solid **1′** adsorbs ethanol in the two step-wise manner (Figure 5). At low pressure regions with a shallow plateau ($p=0$–0.03 atm), the amount of uptake is 2.0 mol mol^{-1} for **1′**. At higher pressure regions ($p=0.03$–0.05 atm), the ethanol vapor adsorption sharply increases and the amount of uptake at near saturation pressure is 3.5 mol mol^{-1} for **1′**. This corresponds to the two EtOH molecules coordinating Zn^{II} ions and four EtOH guest molecules included in the channels per formula unit of **1′**, which is in agreement with the X-ray structure of **1**.

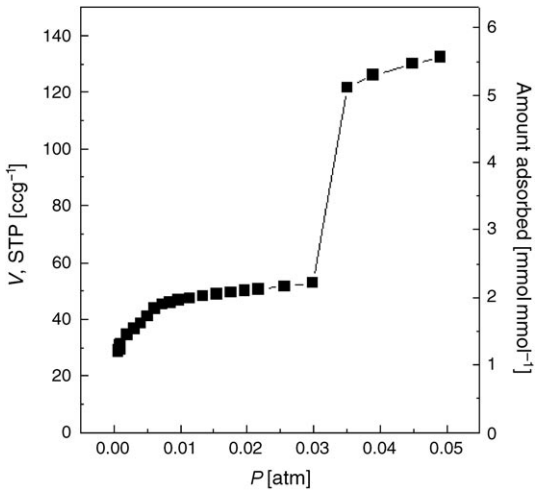

Figure 5. Adsorption isotherm for ethanol vapor at 298 K on solid **1′**.

Conclusion

We have demonstrated by complete X-ray single crystal analyses of **1**, **1′** and **1″** that the metal ions in MOF rearrange the coordination geometry to the thermodynamically

most stable geometry upon removal and rebinding of the coordinating solvent molecules. This is contrary to our general expectation that MOFs would generate vacant coordination sites when coordinating solvent molecules are removed from the metal ions. Despite the coordination flexibility, the present MOF retains its framework structure as well as the single crystallinity during the release and uptake of the coordinating EtOH as well as EtOH guest molecules. The material exhibits permanent porosity and remarkable gas sorption capabilities for N_2, H_2, CO_2, and CH_4 even after loss of coordinating EtOH as well as EtOH guest molecules. The interesting reversible single-crystal dynamics and the significant gas-sorption capabilities of the present MOF can find useful applications in sensors as well as gas storage and/or separation materials.

Experimental Section

General methods: All chemicals and solvents used in the syntheses were of reagent grade and were used without further purification. 4,4′,4″-Nitrilotrisbenzoic acid (H_3NTB) was prepared according to the method previously reported.[42]

Measurements: Infrared spectra were recorded with a Perkin Elmer Spectrum One FT-IR spectrophotometer. UV/Vis diffuse reflectance spectra were recorded on a Perkin Elmer Lambda35 UV/Vis spectrophotometer. Emission spectra were recorded with a Perkin Elmer LS55 luminescence spectrophotometer. Elemental analyses were performed by the analytical laboratory of Seoul National University. Thermogravimetric analysis (TGA) and differential scanning calorimetry (DSC) were performed at a scan rate of 5 °C min^{-1} using TGA Q50 and DSC Q10 of TA instruments, respectively. X-ray powder diffraction (XRPD) data were recorded on a Mac Science M18XHF-22 diffractometer at 50 kV and 100 mA for $Cu_{K\alpha}$ ($\lambda = 1.54050$ Å) with a scan speed of 5° min^{-1} and a step size of 0.02° in 2θ.

$[Zn_3(ntb)_2(EtOH)_2]_n$·4*n*EtOH (1): A EtOH (10 mL) solution of H_3NTB (0.120 g, 3.2×10^{-4} mol) and a EtOH (2 mL) solution of $Zn(NO_3)_2\cdot6H_2O$ (0.160 g, 5.4×10^{-4} mol) were mixed in a Teflon vessel within the autoclave. The vessel was heated at 110 °C for 24 h and then cooled to room temperature. Brown rod-like crystals formed, which were filtered, and washed briefly with EtOH. Yield: 0.153 g, 78 %; FT-IR (KBr pellet): $\tilde{\nu}$ = 1592, 1537 (O-C=O), 3070 (C-H of NTB), 2972 cm^{-1} (C-H of EtOH); UV/Vis (diffuse reflectance spectrum): λ_{max} = 257, 316, 378 (sh), 426 nm (sh); elemental analysis calcd (%) for $Zn_3C_{54}H_{60}N_2O_{18}$ (1221.24): C 53.11, H 4.95, N 2.29; found: C 51.82, H 4.78, N 2.53.

$[Zn_3(ntb)_2]_n$ (1′): Single crystal **1** was introduced in a glass capillary with an open end and was desolvated at 150 °C under 1 Torr for 5 h. After desolvation, drying pistol was filled with dry air (1.0 atm), and then the capillary was taken out, and sealed for X-ray structure determination. For bulk preparation, crystals of **1** were heated at 150 °C under vacuum for 5 h. FT-IR (KBr pellet): $\tilde{\nu}$ = 1595 (O-C=O), 3066 cm^{-1} (C-H of NTB); UV/Vis (diffuse reflectance spectrum): λ_{max} = 259, 315, 385 (sh), 430 nm (sh); elemental analysis calcd (%) for $Zn_3C_{42}H_{24}N_2O_{12}$ (944.74): C 53.39, H 2.56, N 2.97; found: C 51.64, H 3.13, N 2.88.

$[Zn_3(ntb)_2(EtOH)_2]_n$·4*n*EtOH (1″): After the cell parameters of single crystal **1′** were determined in a sealed capillary, one side of the capillary was broken, and then EtOH vapor was allowed to diffuse into the crystal for 3 h. The opening of the capillary was sealed again for collection of the X-ray diffraction data of **1″**. For bulk preparation, **1′** was exposed to EtOH vapor for 3 h, or immersed in EtOH for 5 min.

Gas-sorption study: Gas-sorption isotherms for **1′** were measured on a Quantachrome Autosorb-1 instrument. Solid **1** was dried at 60 °C under vacuum for 2 h. An exactly measured amount of the dried solid was introduced into the gas-sorption apparatus, and evacuated at 30 °C under ca. 10^{-5} Torr for 24 h. Gas sorption isotherms for N_2 and H_2 were monitored at 77 K and those for CO_2 and CH_4 were measured at both 195 K and at 273 K, at each equilibrium pressure by the static volumetric method.

X-ray crystallography: Diffraction data for **1**, **1′**, and **1″** were collected with an Enraf Nonius Kappa CCD diffractometer ($Mo_{K\alpha}$, λ = 0.71073 Å, graphite monochromator). Preliminary orientation matrices and unit cell parameters were obtained from the peaks of the first ten frames and then refined using the whole data set. Frames were integrated and corrected for Lorentz and polarization effects by using DENZO.[43] The scaling and the global refinement of crystal parameters were performed by SCALEPACK.[43] No absorption correction was made. The crystal structures were solved by the direct methods[44] and refined by full-matrix least-squares refinement using the SHELXL-97 computer program.[45] The positions of all non-hydrogen atoms were refined with anisotropic displacement factors. The hydrogen atoms were positioned geometrically and refined using a riding model. For **1** and **1″**, four EtOH guest molecules per formula unit of host framework were refined. The crystallographic data and the selected bond lengths and angles for **1**, **1′**, and **1″** are summarized in Tables 2 and 3.

Table 2. Crystallographic data for **1**, **1′**, and **1″**.

	1	**1′**	**1″**
empirical formula	$Zn_3C_{54}H_{60}N_2O_{18}$	$Zn_3C_{42}H_{24}N_2O_{12}$	$Zn_3C_{54}H_{60}N_2O_{18}$
formula weight	1221.24	944.74	1221.24
space group	*C*2/*c* monoclinic	*C*2/*c* monoclinic	*C*2/*c* monoclinic
a [Å]	15.7334(5)	15.631(4)	15.6988(12)
b [Å]	25.0527(9)	24.948(6)	25.1203(19)
c [Å]	16.8171(4)	16.800(4)	16.5589(13)
β [°]	113.526(2)	113.875(4)	114.7640(10)
V [Å^3]	6077.7(3)	5991(2)	5929.6(8)
Z	4	4	4
ρ_{calcd} [g cm^{-3}]	1.335	1.048	1.368
T [K]	293(2)	293(2)	293(2)
λ [Å]	0.71069	0.71073	0.71073
μ [mm^{-1}]	1.241	1.236	1.272
GOF	1.081	0.753	1.071
F(000)	2528	1904	2528
no. data collected	11257	18648	17996
no. unique data	6955	7001	6823
no. obsd data [$I > 2\sigma(I)$]	5056	2878	5013
no. variables	312	267	348
θ range [°]	2.58–27.51	1.64–28.26	1.64–28.31
R_1[a], wR_2[b] [$I > 2\sigma(I)$]	0.0662, 0.1889	0.0404, 0.0877	0.0645, 0.1882
R_1[a], wR_2[b] (all data)	0.0930, 0.2109	0.1085, 0.0952	0.0893, 0.2033
largest diff. peak/hole, [e Å^{-3}]	0.850, −0.541	0.597, −0.266	1.507, −0.808

[a] $R = \Sigma\,||F_o| - |F_c||/\Sigma\,|F_o|$. [b] $wR(F^2) = [\Sigma w(F_o^2 - F_c^2)^2/\Sigma w(F_o^2)^2]^{1/2}$ where $w = 1/[\sigma^2(F_o^2) + (0.1218P)^2 + (9.45)P]$, $P = (F_o^2 + 2F_c^2)/3$ for **1**, where $w = 1/[\sigma^2(F_o^2) + (0.0381P)^2 + (0.00)P]$, $P = (F_o^2 + 2F_c^2)/3$ for **1′**, and where $w = 1/[\sigma^2(F_o^2) + (0.1036P)^2 + (27.77)P]$, $P = (F_o^2 + 2F_c^2)/3$ for **1″**.

CCDC-612958 (**1**), -612959 (**1′**), and -612960 (**1″**) contain the supplementary crystallographic data for this paper. These data can be obtained free of charge from The Cambridge Crystallographic Data Centre via www.ccdc.cam.ac.uk/data_request/cif.

Table 3. Selected bond lengths [Å] and angles [°] for **1**, **1′**, and **1″**

	1 (original)	**1′** (desolvated)	**1″** (resolvated)
Zn1−O5[a]	1.931(3)	1.924(2)	1.946(4)
Zn1−O6[b]	1.940(3)	1.935(2)	1.947(4)
Zn1−O2	1.957(3)	1.946(2)	1.973(4)
Zn1−O4[c]	2.138(3)	1.943(2)	2.164(3)
Zn1−O7	2.261(5)	–	2.175(5)
Zn2−O1	1.973(3)	1.944(2)	1.974(3)
Zn2−O3[c]	1.951(3)	1.962(2)	1.951(3)
O5[a]-Zn1-O6[b]	138.9 (2)	124.2(1)	141.5(2)
O5[a]-Zn1-O2	110.6(2)	102.8(9)	111.0(2)
O6[a]-Zn1-O2	108.5(2)	104.2(1)	107.0(2)
O5[a]-Zn1-O4[c]	91.7 (2)	106.8(1)	88.7(2)
O6[b]-Zn1-O4[c]	91.0(2)	103.6(1)	89.2(2)
O2-Zn1-O4[c]	103.7(1)	116.0(1)	102.0(1)
O1-Zn2-O1[d]	94.1(2)	95.7(1)	93.1(2)
O1-Zn2-O3[e]	103.3(1)	103.3(1)	102.9(1)
O1-Zn2-O3[f]	115.5(1)	115.6(1)	115.7(1)
Zn1--Zn2	3.593(1)	3.795(1)	3.790(6)
Zn1--Zn1[g]	3.587(1)	3.520(1)	3.485(1)
⧾Ph1-Ph2[h]	77.6(2)	78.5(1)	76.4(2)
⧾Ph1-Ph3[h]	57.3(2)	56.3(1)	56.6(2)
⧾Ph2-Ph3[h]	78.9(2)	76.2(1)	77.2(2)
⧾Ph1-C1[i]	4.9(2)	5.0(1)	2.9(2)
⧾Ph2-C8[i]	10.5(7)	11.5(5)	11.4(7)
⧾Ph3-C15[i]	8.7(8)	17.7(5)	9.1(9)

[a–g] Symmetry relations: [a] $-x$, $1-y$, $-z$. [b] $x-0.5$, $y-0.5$, z. [c] $-x-0.5$, $y-0.5$, $-z+0.5$. [d] $-x$, y, $-z+0.5$. [e] $x+0.5$, $y-0.5$, z. [f] $-x-0.5$, $y-0.5$, $-z+0.5$. [g] $-x-0.5$, $-y+0.5$, $-z$. [h] Dihedral angle between the phenyl rings. [i] The dihedral angle between two least-squares planes involving the noted atoms, as indicated below.

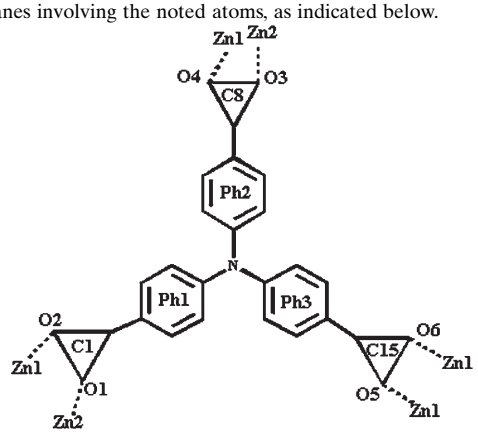

Acknowledgements

This work was supported by the Korea Research Foundation Grant funded by the Korean Government (MOEHRD, Basic Research Promotion Fund) (KRF-2005-084-C00020), and by the SRC/ERC program of MOST/KOSEF (Grant no. R11-2005-008-03002-0), Republic of Korea.

[1] E. Y. Lee, M. P. Suh, *Angew. Chem.* **2004**, *116*, 2858–2861; *Angew. Chem. Int. Ed.* **2004**, *43*, 2798–2801.
[2] E. Y. Lee, S. Y. Jang, M. P. Suh, *J. Am. Chem. Soc.* **2005**, *127*, 6374–6381.
[3] M. Eddaoudi, J. Kim, N. Rosi, D. Vodak, J. Watcher, M. O'Keeffe, O. M. Yaghi, *Science* **2002**, *295*, 469–472.
[4] N. L. Rosi, J. Eckert, M. Eddaoudi, D. T. Vodak, J. Kim, M. O'Keeffe, O. M. Yaghi, *Science* **2003**, *300*, 1127–1129.
[5] A. G. Wong-Foy, A. Matzger, O. M. Yaghi, *J. Am. Chem. Soc.* **2006**, *128*, 3494–3495.
[6] M. P. Suh, J. W. Ko, H. J. Choi, *J. Am. Chem. Soc.* **2002**, *124*, 10976–10977.
[7] H. J. Choi, M. P. Suh, *J. Am. Chem. Soc.* **2004**, *126*, 15844–15851.
[8] H. Kim, M. P. Suh, *Inorg. Chem.* **2005**, *44*, 810–812.
[9] K. S. Min, M. P. Suh, *Chem. Eur. J.* **2001**, *7*, 303–313.
[10] H. J. Choi, T. S. Lee, M. P. Suh, *Angew. Chem.* **1999**, *111*, 1490–1493; *Angew. Chem. Int. Ed.* **1999**, *38*, 1405–1408.
[11] J. W. Ko, K. S. Min, M. P. Suh, *Inorg. Chem.* **2002**, *41*, 2151–2157.
[12] M. Eddaoudi, H. Li, O. M. Yaghi, *J. Am. Chem. Soc.* **2000**, *122*, 1391–1397.
[13] K. S. Min, M. P. Suh, *J. Am. Chem. Soc.* **2000**, *122*, 6834–6840.
[14] H. J. Choi, M. P. Suh, *Inorg. Chem.* **2003**, *42*, 1151–1157.
[15] O. M. Yaghi, H. Li, *J. Am. Chem. Soc.* **1996**, *118*, 295–296.
[16] C. D. Wu, A. Hu, L. Zhang, W. Lin, *J. Am. Chem. Soc.* **2005**, *127*, 8940–8941.
[17] T. Uemura, R. Kitaura, Y. Ohta, M. Nagaoka, S. Kitagawa, *Angew. Chem.* **2006**, *118*, 4218–4222; *Angew. Chem. Int. Ed.* **2006**, *45*, 4112–4116.
[18] B. Gomez-Lor, E. Gutierrez-Puebla, M. Iglesias, M. A. Monge, C. Ruiz-Valero, N. Snejko, *Chem. Mater.* **2005**, *17*, 2568–2573.
[19] M. Albrecht, M. Lutz, A. L. Spek, G. van Koten, *Nature* **2000**, *406*, 970–974.
[20] J. A. Real, E. Andrés, M. C. Muñoz, M. Julve, T. Granier, A. Bousseksou, F. Varret, *Science* **1995**, *268*, 265–267.
[21] L. G. Beauvais, M. P. Shores, J. R. Long, *J. Am. Chem. Soc.* **2000**, *122*, 2763–2772.
[22] M. P. Suh, H. R. Moon, E. Y. Lee, S. Y. Jang, *J. Am. Chem. Soc.* **2006**, *128*, 4710–4718.
[23] H. R. Moon, J. H. Kim, M. P. Suh, *Angew. Chem.* **2005**, *117*, 1287–1291; *Angew. Chem. Int. Ed.* **2005**, *44*, 1261–1265.
[24] H. Li, M. Eddaoudi, T. L. Groy, O. M. Yaghi, *J. Am. Chem. Soc.* **1998**, *120*, 8571–8572.
[25] H. Li, C. E. Davis, T. L. Groy, D. G. Kelley, O. M. Yaghi, *J. Am. Chem. Soc.* **1998**, *120*, 2186–2187.
[26] T. M. Reineke, M. Eddaoudi, M. Fehr, D. Kelley, O. M. Yaghi, *J. Am. Chem. Soc.* **1999**, *121*, 1651–1657.
[27] B. Chen, N. W. Ockwig, A. R. Millward, D. S. Contreras, O. M. Yaghi, *Angew. Chem.* **2005**, *117*, 4823–4827; *Angew. Chem. Int. Ed.* **2005**, *44*, 4745–4749.
[28] B. Chen, M. Eddaoudi, T. M. Reineke, J. W. Kampf, M. O'Keeffe, O. M. Yaghi, *J. Am. Chem. Soc.* **2000**, *122*, 11559–11560.
[29] P. D. C. Dietzel, Y. Morita, R. Blom, H. Fjellvag, *Angew. Chem.* **2005**, *117*, 6512–6516; *Angew. Chem. Int. Ed.* **2005**, *44*, 6354–6358.
[30] C.-L. Chen, A. M. Goforth, M. D. Smith, C.-Y. Su, H.-C. zur Loye, *Angew. Chem.* **2005**, *117*, 6831–6835; *Angew. Chem. Int. Ed.* **2005**, *44*, 6673–6677.
[31] D. Sun, S. Ma, Y. Ke, D. J. Collins, H.-C. Zhou, *J. Am. Chem. Soc.* **2006**, *128*, 3896–3897.
[32] Q. Yang, D. J. Zhong, *J. Phys. Chem. B* **2006**, *110*, 655–658.
[33] S. S. Kaye, J. R. Long, *J. Am. Chem. Soc.* **2005**, *127*, 6506–6507.
[34] M. Dinca, J. R. Long, *J. Am. Chem. Soc.* **2005**, *127*, 9376–9377.
[35] A. L. Spek, *PLATON99, A Multipurpose Crystallographic Tool*, Utrecht University: Utrecht, The Netherlands, **1999**.
[36] A. Vishnyakov, P. I. Ravikovitch, A. V. Neimark, M. Bulow, O. M. Wang, *Nano Lett.* **2003**, *3*, 713–718.
[37] J. Y. Lee, J. Li, J. Jagiello, *J. Solid State Chem.* **2005**, *178*, 2527–2532.
[38] G. Horvath, K. Kawazoe, *J. Chem. Eng. Jpn.* **1983**, *16*, 470–475.
[39] National Institute of Standards and Technology homepage. http://webbook.nist.gov/chemistry/ (accessed February 2006)
[40] J. L. Atwood, L. J. Barbour, A. Jerga, *Angew. Chem.* **2004**, *116*, 3008–3010; *Angew. Chem. Int. Ed.* **2004**, *43*, 2948–2950.
[41] A. R. Millward, O. M. Yaghi, *J. Am. Chem. Soc.* **2005**, *127*, 17998–17999.
[42] S. Dapperheld, E. Steckhan, K. -H. G. Brinkhaus, T. Esch, *Chem. Ber.* **1991**, *124*, 2557–2567.
[43] Z. Otwinowsky, W. Minor in *Processing of X-ray Diffraction Data Collected in Oscillation Mode, Methods in Enzymology, Vol. 276*

(Eds.: C. W. Carter, R. M. Sweet), Academic Press, New York, **1996**, pp. 307–326.
[44] G. M. Sheldrick, *Acta Crystallogr. Sect. A* **1990**, *A46*, 467.
[45] G. M. Sheldrick, SHELXL97, Program for the crystal structure refinement, University of Göettingen, Göettingen (Germany), **1997**.

Received: October 27, 2006
Published online: February 22, 2007

